CANADA
DEPARTMENT OF ENERGY, MINES AND RESOURCES
Observatories Branch

PUBLICATIONS

of the

DOMINION OBSERVATORY

OTTAWA

Volume XXV • No. 13

THE 22.25 MHz RADIO TELESCOPE AT THE DOMINION RADIO ASTROPHYSICAL OBSERVATORY

C. H. Costain, J. D. Lacey and R. S. Roger

ROGER DUHAMEL, F.R.S.C.
QUEEN'S PRINTER AND CONTROLLER OF STATIONERY
OTTAWA 1969

CONTENTS

PAGE

Abstract 327
Introduction 327
The *T*-Configuration 328
The Central Overlap Region 329
The 22.25 MHz Array 329
General Description 329
Basic Element 330
The Reflecting Screen 330
The East-West Array 330
The North-South Array 331
The Phasing System 331
Receiving and Auxiliary Equipment 332
Calibration and Performance 332
Discussion 334
Acknowledgments 334
References 334

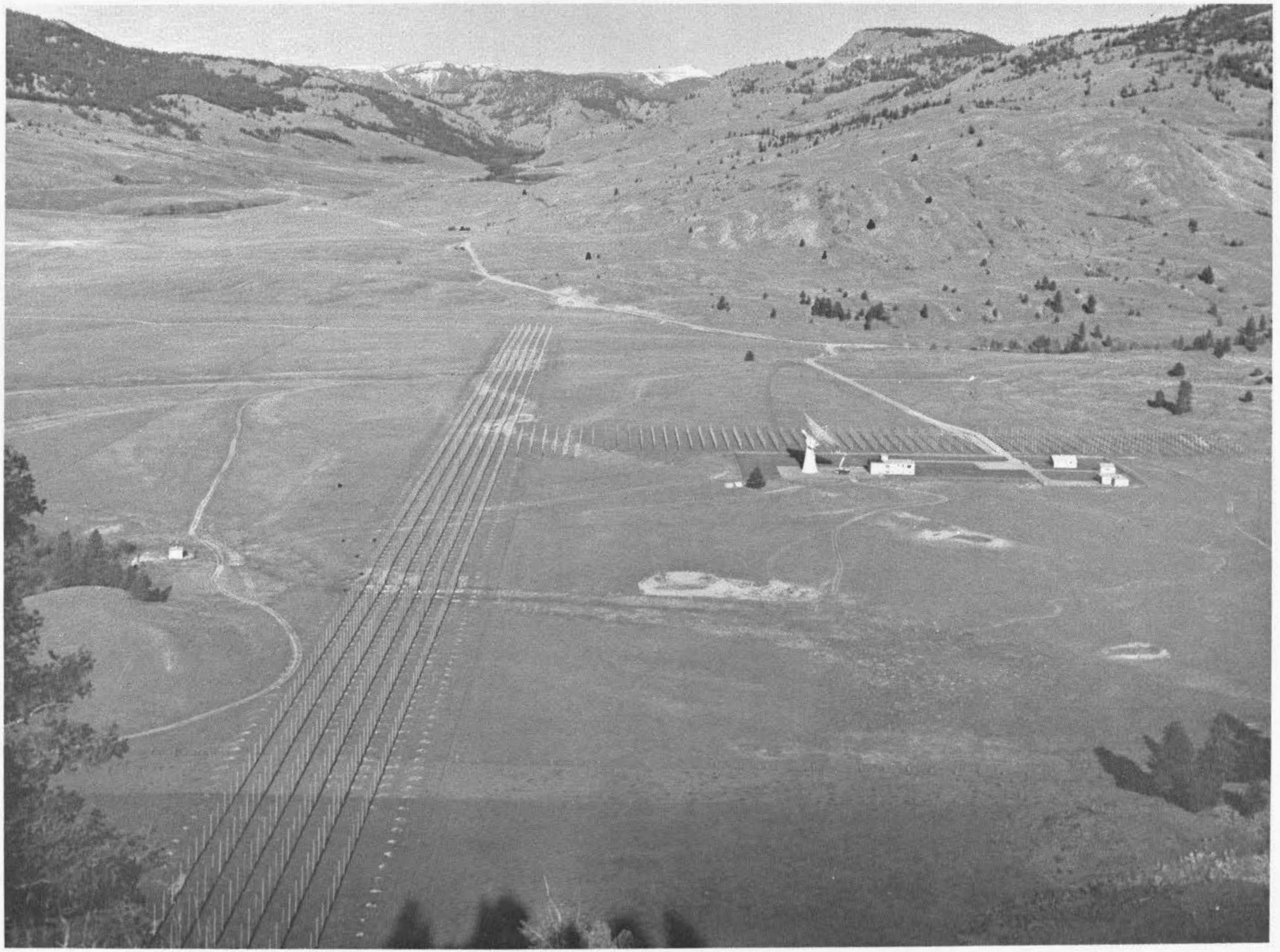

Figure 1. A photograph of the 22.25 MHz array taken from the east.

THE 22.25 MHz RADIO TELESCOPE AT THE DOMINION RADIO ASTROPHYSICAL OBSERVATORY

C.H. COSTAIN, J.D. LACEY and R.S. ROGER

ABSTRACT – Radio telescopes of the *T* and Cross configurations are compared and their relative merits discussed.

A large *T* array built at the Dominion Radio Astrophysical Observatory for radio astronomical observations at 22.25 MHz ($\lambda = 13.5$ m) is described. It consists of 624 full-wave dipoles above a reflecting screen 65,000 m^2 in area. The dipoles are arranged in an east-west section of dimensions $96\lambda \times 2.5\lambda$ and in a north-south section $32.5\lambda \times 4\lambda$. The instrument has a pencil-beam response of $1.^\circ 1 \times 1.^\circ 7$ at the zenith. Simultaneous observations at five adjacent declinations are made with a time-sharing technique.

Observations commenced in 1965 and will provide flux density measures for 400 to 500 radio sources down to a limiting flux density of $30 \times 10^{-26} Wm^{-2} Hz^{-1}$. A map of the galactic background radiation from the sky north of -20° declination is being prepared.

RÉSUMÉ – Les auteurs passent en revue les radiotélescopes constitués de réseau en forme de *T* et de réseau croisé et présentent les avantages de chacun.

Ils décrivent un grand réseau en forme de *T* construit à l'Observatoire fédéral de radio-astrophysique et destiné à des observations astronomiques sur la bande de fréquences de 22.25MHz ($\lambda = 13.5$ m). Le réseau est constitué de 624 dipoles à onde complète placés au-dessus d'un écran réflecteur d'une superficie de 65,000 mètres carrés. Les dipôles sont disposés sur un aérien orienté en direction est-ouest et de dimension correspondant à 96λ sur 2.5λ et sur un autre aérien en direction nord-sud de dimension correspondant à 32.5λ sur 4λ. La réponse du lobe principal est de $1.^\circ 1$ sur $1.^\circ 7$ au zénith. On peut procéder à des observations simultanées à cinq déclinaisons adjacentes grâce à une technique de partage du temps.

Les observations ont commencé en 1965 et elles fourniront des mesures de la densité de flux pour 400 à 500 radiosources à partir d'une densité de $30 \times 10^{-26} Wm^{-2} Hz^{-1}$. On prépare pour tout l'hémisphère boréal du ciel et jusqu'au 20^e degré de déclinaison sud une carte des émissions continues de la galaxie.

Introduction

Instrumental development in radio astronomy has been directed primarily towards the achievement of systems of high resolving power. With the great improvements in high-frequency receivers and antennas, the trend at most observatories has been towards the use of higher and higher frequencies where adequate resolving power may be obtained with structures of moderate size. Apart from the pioneer work of Shain (1958, 1961) there has until recently been a relative neglect of the low-frequency end of the radio astronomy spectrum.

Observations at low frequencies are, of course, required to extend our knowledge of the radio spectra of all sources of radio emission. Some studies, however, such as the examination of the complex structure of the galactic continuum radiation, are best carried out at the longer wavelengths where the intensities are very high. The low-frequency radio telescope is the most sensitive detector of the diffuse clouds of ionized hydrogen which appear in absorption against the bright galactic background (see Figure 12).

When the present instrument was planned, the largest low-frequency array in the northern hemisphere was the 38 MHz Moving-*T* at the Mullard Radio Astronomy Observatory, Cambridge (Costain and Smith, 1960). An operating frequency near 20 MHz was therefore desirable to extend spectral measurements about an octave. The choice of 22.25 MHz ($\lambda = 13.5$ m) was made after a careful study of the incidence of radio interference in nearby bands.

Because of the almost complete absence of previous measurements at this frequency, it was decided to build a general purpose telescope similar to the Mills Cross (Mills, *et al.*, 1958). In these systems, the voltage outputs of two long thin orthogonal arrays are multiplied together to produce the desired 'pencil-beam' response. The 22 MHz instrument is, in fact, a *T*-shaped array. The $96\lambda \times 2.5\lambda$ east-west arm and the $32.5\lambda \times 4\lambda$ north-south arm combine to provide a response of $1.^\circ 1 \times 1.^\circ 7$ at the zenith.

Several large interferometer systems, as opposed to pencil-beam instruments, are now being used to study small-diameter radio sources at low frequencies: the 26.3 MHz compound grating interferometer at Clarke Lake, U.S.A. (Erickson, 1965), and the broad-band arrays (10-25 MHz, 20-40 MHz) in the U.S.S.R. (Bazelyan, *et al.*, 1965; Brouk, *et al.*, 1967). The extremely favourable observing conditions encountered during early observations with parts of the 22 MHz array, prompted the decision, late in 1963, to build a similar instrument to operate at a frequency near 10 MHz (Galt, *et al.*, 1967). These arrays at the Dominion Radio Astrophysical Observatory are, at present, unique facilities in this frequency range in that they also permit observations of the extended features of the Galaxy.

This paper is devoted to a discussion of *T*-shaped antenna systems and a detailed description of the design and performance of the 22.25 MHz array. Brief descriptions of the instrument have appeared elsewhere, (Costain, 1962; Galt and Costain, 1965).

The *T*-Configuration

The equivalence of "perfect" Cross and *T* system has been discussed in detail elsewhere (Blythe, 1957; Ryle and Hewish, 1960; Mills, 1963). It can be easily demonstrated by reference to Figure 2(a). Since the output of a *T* or Cross is the product of the outputs of the two orthogonal arrays, the only relevant spacial components are those between the elements of one array and those of the other. It may be seen that all element spacings and orientations present in the uniform aperture are contained in the Cross and *T*, with each component appearing twice in the Cross configuration (c.f. the arrows in Figure 2(a)). The *L*-configuration, where a further arm of the Cross has been removed, does not contain all necessary element orientations. With an appropriate weighting of the elements, the Cross or *T* can precisely duplicate the response beam of the uniform aperture. However, rather than discard half of one arm of the Cross with the resultant loss in sensitivity, the alternative arrangement shown in 2(b) where the elements of the south arm are placed to provide a north-south arm of twice the width, may be used and is identical in both resolving power and sensitivity to the Cross. It is this *T*-configuration which will be considered in subsequent discussion.

Both systems are, of course, unfilled apertures and as such are less sensitive than the uniform aperture of equivalent resolving power. Ryle and Hewish (1960) have expressed this effect in terms of an efficiency parameter E, which is the ratio of the effective collecting area of the system A_{eff} to that of the equivalent uniform aperture A. For the *T*-configuration shown in Figure 2(b), this is given by

$$E = \frac{A_{eff}}{A} = \sqrt{\frac{2\,d_1 d_2}{D_1 D_2}} = \frac{T_a}{T_b} \qquad (1)$$

where T_a is the aerial temperature (neglecting losses) obtained when the system is used to observe a region of uniform brightness, T_b. The major design parameters, therefore, for a given resolution, are the array widths d_1 and d_2, with the optimum values being those which ensure that the system has sufficient sensitivity to reach the confusion limit for point source observations.

Most practical systems employing the *T*-configuration have used it as an interim phase in the development of a Cross system (Bracewell and Swarup, 1961) or have used the aperture synthesis technique (Blythe, 1957; Costain and Smith, 1960; Crowther and Clarke, 1966). Discussion has centred largely on the sensitivity of the *T* to errors in the excitations of the array elements (Mills, 1963). However, the *T* offers some unique advantages over the Cross which merit serious consideration. The *T*-configuration of Figure 2(b) is superior to the Cross in three respects:

1. The number of phasing switches, multibeam elements, preamplifiers, cables, etc., needed for the north-south arm is reduced by half.

2. The extent in hour angle over which the side-lobes of the east-west array are significant is reduced by half because of the increased width of the north-south array.

3. The maximum north-south dimension required at the antenna site, for a given beamwidth, is also reduced by half.

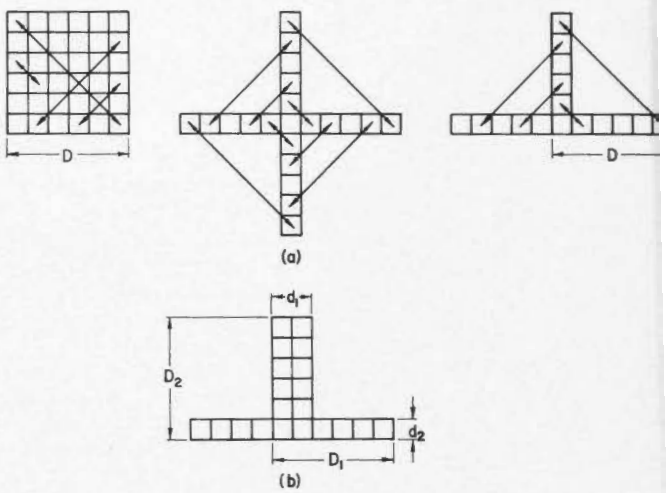

Figure 2. (a) Apertures of equal resolving power. (b) A *T*-configuration equivalent to the Cross in both resolving power and sensitivity.

Perhaps the major advantage of the *T*-configuration lies in the economies that result from halving the feeder and phasing arrangements of the north-south array. As mentioned above, for reasons of sensitivity, the area of the north-south array and therefore the cost of the basic structure, are likely to be similar in the *T* and Cross systems. The phasing and multibeam arrangements necessary to provide beam scanning in declination, however, remain a major cost factor and perhaps the most difficult engineering problem in the design of large arrays. For any large instrument, it seems likely that a monitor system to maintain the accuracy of the excitations of the north-south array can be installed for a small fraction of the cost of duplicating the entire north-south feeder system.

The side-lobes of unfilled apertures such as the *T* or Cross are always troublesome because these instruments are used to examine a universe populated with many bright radio sources. The side-lobes in hour angle are reduced to negligible values at angles beyond the first zero of the east-west response of the north-south array. The reduced angular extent of the hour angle side-lobes mitigates, to a large extent, the slightly larger declination side-lobes discussed below.

The *T* is inferior to the Cross in its greater sensitivity to errors in the excitations of the elements of the north-south array. These errors produce spurious side-lobe responses in declination and may be divided into two classes, random and systematic, whose effects are considered separately.

Errors in measurement in the adjustment of the excitations will result in random errors in amplitude and phase. In general, these errors will have a mean value of zero and rms values dependent to a large extent on the time and effort expended to reduce them. For a given rms error, the *T* system would be expected to have a declination side-lobe level $\sqrt{2}$ larger simply because only half the number of independent elements are used (Mills, *et al.*, 1958).

A more serious effect results from a systematic differential phase shift between the north-south and east-west arrays. This is illustrated in Figure 3 which shows the asymmetric side-lobes and the 0.14 beamwidth collimation error due to a gross differential phase error of 20°. Avoidance of this type of error requires some sort of system to monitor the differential phase. This is easily accomplished by the injection of a test signal into the overlap region common to both arrays.

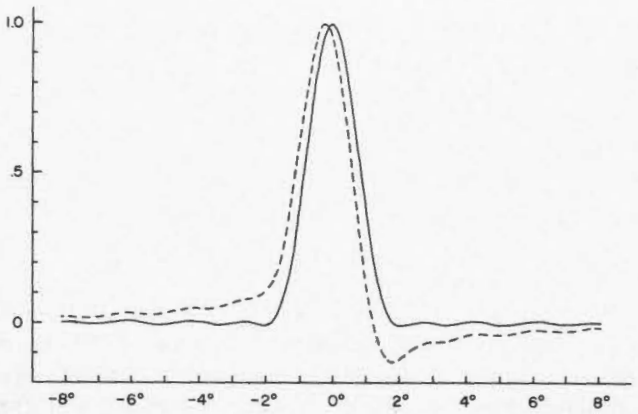

Figure 3. The declination polar diagram of a *T* with differential phase errors of 0° (solid line) and 20° (dashed line).

The Central Overlap Region

One of the design problems in *T* and Cross systems is encountered in the region where the two arms intersect. In the original Mills Cross (Mills, *et al.*, 1958), the central dipoles of the east-west arm were removed. This results in a negative system response, elongated in the east-west plane. A portion of the output of the north-south arm, which had a similar though far from identical response, was added as compensation. Although this method worked well for a uniform background or point sources, it was subject to large errors when the system was used to observe intermediate broad components such as those encountered near the galactic plane.

A different technique, which offers a much more satisfactory solution, positions the elements in the overlap region so that they may be considered to be part of either array. Their outputs are divided with hybrid networks and are fed, with the appropriate weighting, into the feeder systems of both arrays. The output of the system then contains spacial Fourier components down to zero spacing and therefore precisely reproduces a pencil-beam response.

This method was used with the 10 MHz and 22 MHz arrays at the Dominion Radio Astrophysical Observatory.

The 22.25 MHz Array

General Description

The 22.25 MHz array is located near Penticton, British Columbia, Canada, at the Dominion Radio Astrophysical Observatory (longitude = 119°37′08″W; latitude = 49°19′14″N). It is a *T*-shaped array of 624 full-wave dipoles; 368 in the E-W arm, 240 in the N-S arm, and 16 common to both arms. The dipoles are polarized in the E-W direction. A full reflecting screen (area ~ 65,000 m^2) is mounted $\lambda/8$ below the dipoles and the entire structure is supported on a grid of 1698 wooden poles. The plane of the array was adjusted for the best average fit to the terrain. It was therefore necessary to skew the axis of the array slightly from the E-W direction in order that the axial plane of the E-W arm pass through the north celestial pole. The dimensions of the system

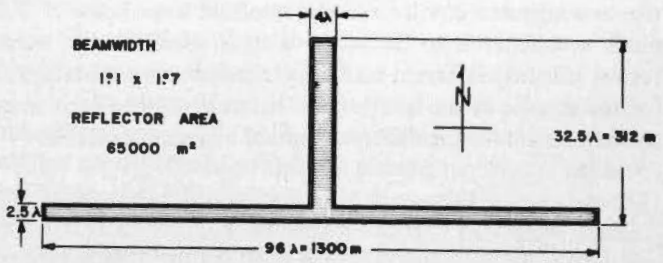

Figure 4. A schematic diagram of the 22.25 MHz array.

are shown in Figure 4 and Figure 1 is a photograph of the array taken from the east. At the zenith, the instrument has an elliptical beam with half-power widths of 1°.1 in hour angle and 1°.7 in declination.

The outputs of the E-W and N-S arms are carried by coaxial cables to preamplifiers located at the centre of each arm and from there to the main observatory building. The signals are then amplified and correlated using the standard phase-switching technique. They are then integrated, digitized and punched on cards.

The array can be phased north and south of the zenith along the meridian. This phasing to any declination is accomplished by means of remotely-controlled switches operated from the main observatory building. A rapid-phasing network operating on a time-sharing basis, provides quasi-simultaneous observations of five adjacent declinations.

At 22 MHz, the mean sky brightness temperature of the order of 30,000°K completely dominates the receiver noise. Losses of 10 db may be tolerated with negligible deterioration in signal-to-noise, permitting the use of inexpensive coaxial cable for the bulk of the feeder system and the use of resistive attenuators for the grading of the aperture.

The array has an efficiency, as defined by Equation (1), of approximately 10 per cent, a value considerably higher than that usually employed (Shain, 1958; Mills, *et al.*, 1958). The effective collecting area of the instrument is therefore

$$A_{eff} \approx 30{,}000 \text{ m}^2 \qquad (2)$$

This efficiency permits observation of areas of low surface brightness away from the galactic plane. The collecting area is more than adequate for the detection of sources with flux densities near the confusion limit of $S = 33 \times 10^{-26} \mathrm{Wm}^{-2}\mathrm{Hz}^{-1}$ (1 source per 20 beam areas). Under ideal observing conditions, the system is capable of providing flux density measures for approximately 600 radio sources.

Basic Element

The basic element in the array consists of two full-wave dipoles $\lambda/8$ above the reflecting screen (see Figure 5). A broad-band dipole (impedance 2000 ohms resistive) was constructed from two loops of wire. A vertical twin line couples the dipole to the feeders below the reflecting screen. A $\lambda/4$ shorted stub and a $\lambda/4$ transformer permit adjustment of the impedance to 400 ohms. Sections of 400-ohm line couple the two adjacent dipoles and the resultant impedance of 200 ohms is converted to 50 ohms with a coaxial balun transformer. Slightly different matching transformers were required for the dipoles in the interior and exterior rows of each array to compensate for the different mutual impedance effects.

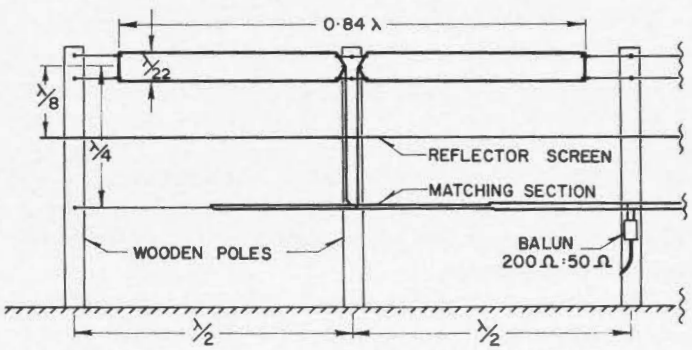

Figure 5. The basic element of the array. For simplicity, only one of the two full-wave dipoles is shown.

The Reflecting Screen

The ground plane of the array is accurately defined by a full reflecting screen which extends $\lambda/2$ beyond the dipoles in the N-S direction. It consists of fine galvanized steel wires aligned parallel to the dipoles and spaced $\lambda/22$ apart. The area of the reflecting screen is approximately 65,000 m^2. The screen is supported by heavy guy wires which also serve to accurately position the self-supporting wooden poles.

The East-West Array

In the E-W arm, the elements are arranged in four rows. Each row has three groups of 32 full-wave dipoles. The rows are spaced $\lambda/2$ apart, and to permit phasing in the N-S direction, each row has its own feeder system as shown in Figure 6. To preserve the bandwidth of the system, a binary branching (Christmas tree) feeder network is used throughout. This provides an identical cable path of about $62\lambda_c$ from each dipole to the central junction. Of this length, $50\lambda_c$ is composed of phase-stable coaxial cable. At each junction, a coaxial matching section converts the impedance to 50 ohms. The coupling of the four rows in the N-S plane is also done with a branching network with phasing switches (see section on 'The Phasing System') installed at each junction. Originally this was done only at the centre of the array. More recently, to reduce system losses, a branching network and phasing switches were placed at points shown at *A* in Figure 6. The three sections of the array are then coupled to the central point with single lengths of less lossy cable.

Systems such as the *T* or Cross require a severe apodization of their apertures to reduce side-lobe responses. The excitation functions used are shown in Figure 7. For convenience, a common grading attenuator is used for each group of four dipoles (positions shown with X's in Figure 6). A uniform illumination is used in the N-S plane. The grating responses that would normally result from this staircase function fall on the zeros of the response of the 4λ aperture of the N-S array. This excitation function gives the E-W arm a

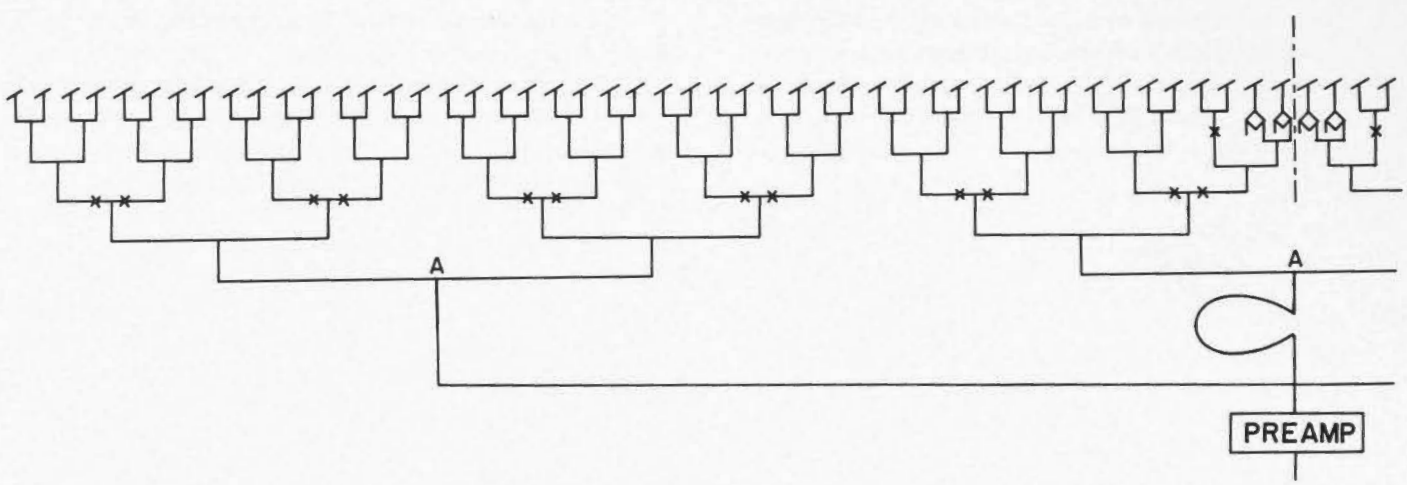

Figure 6. The feeder system for one row of the E-W array. The system is symmetrical about the dashed line. The diamonds indicate the hybrid networks which permit the dipoles in the overlapping region to be shared by both arrays. Grading attenuators are shown as X's.

voltage response with a half-width of 1°.1 in hour angle, a negative first side-lobe of 1 per cent, and remaining side-lobes less than 1 per cent.

When the E-W arm is used by itself in a total power system, it has a half-power beamwidth of 0°.8 by 26° at the zenith.

The North-South Array

The N-S arm consists of 64 rows spaced $\lambda/2$ apart, each with four full-wave dipoles. The four dipoles are coupled together and each row is then connected into the N-S feeder system shown in Figure 8. The total cable path to each dipole is made up of the same length and type of cable used in the E-W array to eliminate differential temperature effects.

To point the beam of an array employing a branching feeder system, the relative phases must be altered at each 2:1 junction. The phasing system is discussed in detail in the following section. However, the phasing of adjacent rows also imposes impedance matching problems because of the large mutual coupling at the $\lambda/2$ spacing.

When the relative phase of two adjacent rows was rotated through 360°, the junction impedance traced out an approximate cardioid pattern on a Smith impedance chart. By adjusting the dipole matching transformers and the lengths of cable between the dipoles and the junction, it was possible to arrange the pattern very close to the unit circle for all phasings except those corresponding to extreme zenith angles. Therefore, a single reactive stub for each phase increment was sufficient to make the junction impedance resistive with a maximum VSWR of 1.3. Because of circuit losses, further concessions to mutual effects at succeeding junctions were not required.

The aperture illumination of the N-S arm is uniform in the E-W plane and follows the function given in Figure 7 in the N-S plane. The zero order component from the overlap region of a *T*-configuration must appear with half the weight of the higher order spacial components to reproduce the component weighting of a uniform aperture. The computed voltage response for this function has a half-width of 1°.7 sec Z, where Z is the zenith angle. The first side-lobe is −1 per cent and all remaining side-lobes are less than 1 per cent.

When used alone as a total power array, the N-S arm has a response with a beamwidth in declination of 2°.1 sec Z and broad, low-level wings. The E-W beamwidth is 14°.

Initially, the desired illumination was achieved with resistive attenuators. In a recent modification coincident with the installation of the rapid-phasing switches described in the following section, a combination of attenuators and coaxial power dividers at the major junctions was used to achieve the same excitation with less over-all attenuation.

The Phasing System

As mentioned previously, the phasing of a branching feeder network requires the installation of a phasing switch at each junction. The main phasing system of the 22 MHz array employs three switches in the E-W arm and 63 switches in the N-S arm.

The phasing switches have 16 positions, each position corresponding to the insertion of an independent length of cable. The use of independent lengths of cable permits the introduction of a unique matching stub for each position of the switches used to phase the adjacent rows of dipoles. The cable lengths vary from 0 to $15\lambda/16$ in increments of $\lambda/16$ or 22°.5. The phase of any row can therefore be adjusted with a maximum error of ±11°. For survey work, the beam positions can be chosen so that the phasing required in the last three stages of the feeder system is an exact multiple of $\lambda/16$. The systematic errors introduced in the first two stages due to the incremental nature of the phase adjustment produce a phase modulation along the aperture with periods of 1λ and 2λ. The corresponding grating responses lie on the zeros of the N-S beam of the E-W array and are rejected.

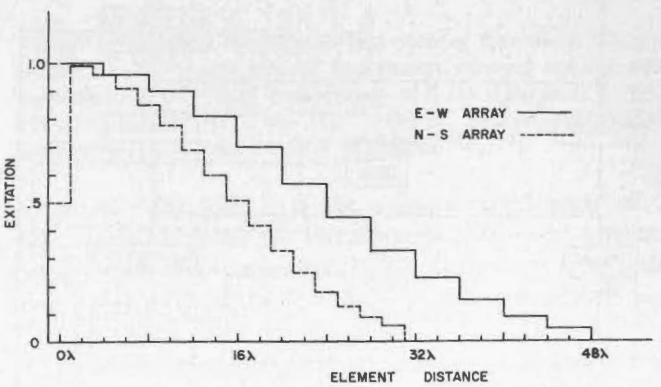

Figure 7. The excitation function for the E-W and N-S arrays.

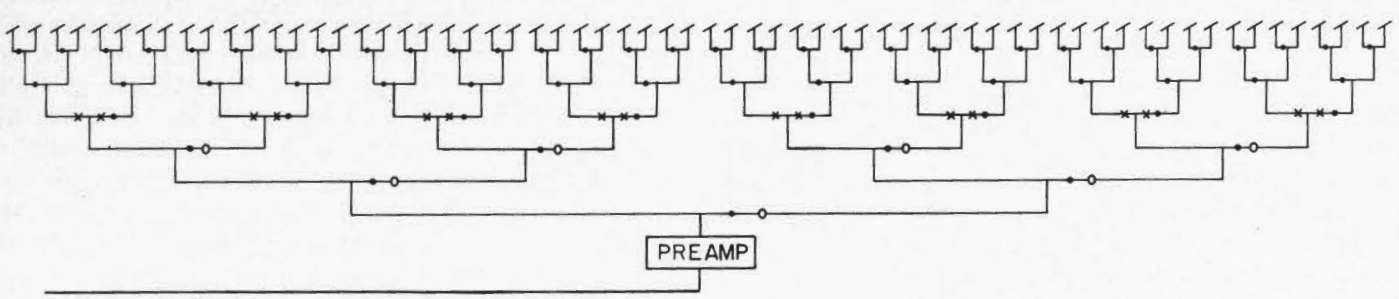

Figure 8. The feeder system of the N-S array: • main phasing switches, ○ rapid phasing switches, X grading attenuators.

Since the switches at any one level in the feeder system require a common phase increment, they are coupled to drive one another in series. By setting the two master switches of the E-W array and the six of the N-S array to tabulated values, it is possible to rapidly point the beam of the instrument to any desired zenith angle in the N-S plane. The switches are driven by rotary solenoids with binary-coded master and slave wafers that permit selection of unique switch positions. Indicator lamps on the control panel and on individual switch housings provide an immediate indication of switch failure.

To permit faster sky coverage for mapping observations and position measurements for point sources, a rapid-phasing network has recently been added. The system operates on a time-sharing basis and provides simultaneous coverage of five adjacent declinations. Seven fast-acting crystal diode switches placed as shown in Figure 8, serve to shift the beam through angles of 0, ±0.263 and ±0.526 beamwidths (0°, ±0°.45, ±0°.90 at the zenith). The beam is pointed to each position four times in each integration period, permitting the observing intervals for each beam position to be arranged symmetrically around the same mean observing time.

Receiving and Auxiliary Equipment

The receivers and associated equipment used with the 22 MHz telescope are illustrated in Figure 9. The preamplifiers are located at the centre of each arm. The remaining units shown are all in the control room of the main observatory building.

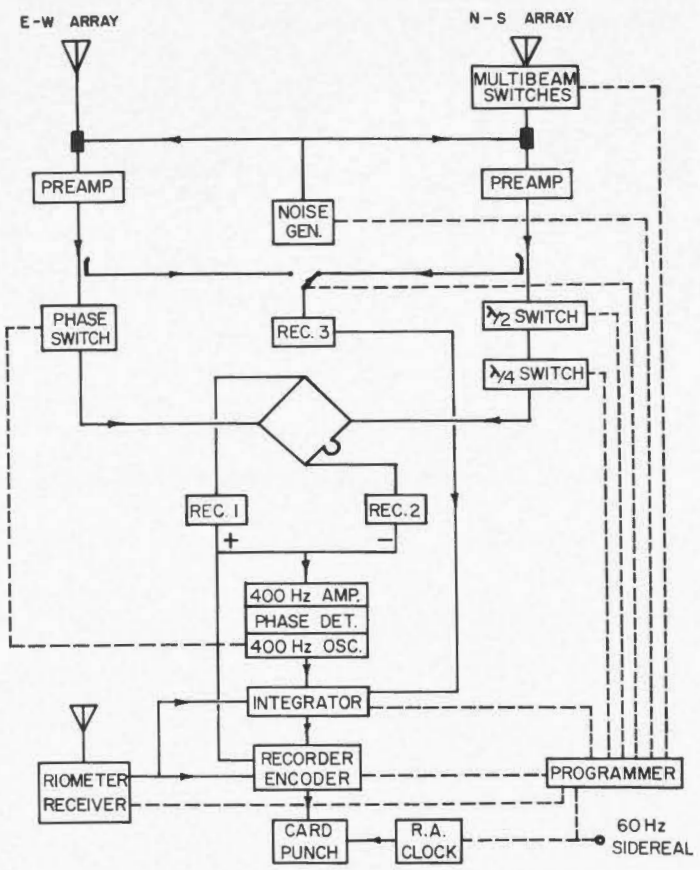

Figure 9. A block diagram of the 22.25 MHz Receiving System. Solid lines indicate signal paths. Dashed lines show control paths.

The receivers used are extremely gain-stable, stagger-tuned amplifiers. They have a flat pass-band of 300 kHz centred on 22.25 MHz with a gain that may be varied from 60 db to 120 db. The correlation is done using the standard phase switching technique developed by Ryle (1952). The use of receivers 1 and 2 to detect both the in-phase and anti-phase components improves the signal-to-noise by $\sqrt{2}$ and greatly aids in the suppression of interference incident on only one of the arms (Scott, *et al.*, 1961). Receiver 3 is used to monitor the total power outputs of the two arms.

The entire system is controlled by the programmer which permits unattended, automatic operation. It consists of a solid-state clock which is driven at the sidereal rate and synchronized to the right ascension clock, and solid-state logic circuits which generate the pulse trains required in the various parts of the system. The intensities for the five beam positions, the total powers from the two arrays, and the riometer output are recorded digitally. Provision is made for 30-second ($\delta<60°$) or 60-second ($\delta>60°$) integration periods and single or multibeam operation.

The $\lambda/2$ switch reverses the phase of the correlated signal for half of each integration period. A synchronous reversal of the integrator input ensures that only the correlated component is recorded, completely independent of any DC drifts that might develop in the system. The $\lambda/4$ switch is used only for testing; it provides a null indication of equal phase paths for the calibration, and for the arrays when a test signal is injected into the overlap region (c.f. section on 'The *T*-configuration'). Both switches employ coaxial reeds and have a low VSWR and a phase insertion accurate to better than 1°.

A diode noise generator inserts a stable, correlated calibration signal into the system during every second integration period. This provides a continuous measure of sensitivity and ensures the long-term continuity of the observations.

A 22.25 MHz riometer, connected to a separate cross-dipole antenna, continuously monitors the ionospheric absorption.

Calibration and Performance

An absolute calibration is particularly important for a large radio astronomy array operating at a frequency where few previous measurements have been made. A method which relates the system gain to that of a standard dipole was developed by Little (1958) for calibration of the original Mills Cross. A standard dipole has been constructed for the 22 MHz array but only preliminary measurements have been made.

An alternative method, which has been used to provide an interim calibration, relates all measurements to the flux density of the radio source *Cygnus A* (S = 29,000 $Wm^{-2}Hz^{-1}$). This is the only source for which a 22 MHz value of sufficient accuracy is available (Kellermann, 1964) and this provides a measure of the instrument sensitivity near the

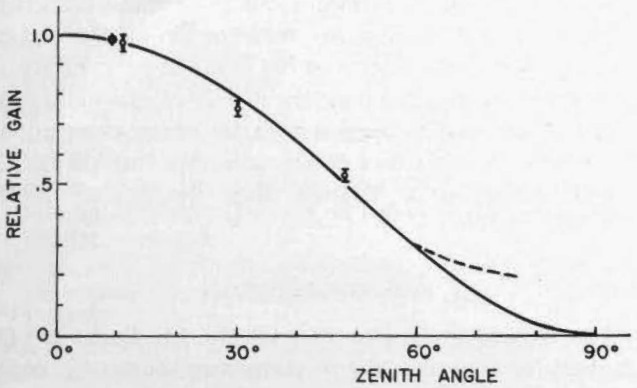

Figure 10. The relative gain of the 22.25 MHz Array as a function of zenith angle: – isolated element, • *Cygnus A* (3C 405), ○ mean of weaker sources in zenith angle zones $0^\circ - 20^\circ$, $20^\circ - 40^\circ$, $40^\circ - 60^\circ$.

zenith. To extend this calibration to other zenith angles, one may use flux densities obtained by extrapolation for those sources which have well defined spectra down to 38 MHz. For the present work, the spectra have been determined from the 38 MHz and 178 MHz flux densities of the Mullard Observatory (Williams, *et al.*, 1966; Gower, *et al.*, 1967; Pilkington and Scott, 1965) and the 750 MHz and 1400 MHz values of the National Radio Astronomy Observatory (Pauliny-Toth, *et al.*, 1966). The ratio of flux densities measured in terms of the zenith calibration to the extrapolated flux densities was calculated for 98 sources. The results have been grouped for three zenith angle zones, $Z = 0^\circ$ to 20°, 20° to 40°, and 40° to 60°. The mean ratios are shown as the circles in Figure 10 together with the point for *Cygnus A*. The error bars shown are probable errors and are approximately 3 per cent.

The response of an isolated element, $\lambda/8$ above a reflecting screen, as a function of zenith angle, i.e.,

$$A(Z) = 2A_0 \sin^2\left(\frac{\pi}{4}\cos Z\right) \tag{3}$$

is shown by the solid line in Figure 10.

The excellent agreement of the results from the fainter sources near the zenith with the *Cygnus A* calibration suggests that the method is reliable. There is no evidence for departures from the isolated element response given by Equation (3) for zenith angles less than 60°.

A possible departure for very large zenith angles, shown as the dashed curve in Figure 10, is suggested by observations of a few southern sources. Some deviation of this sort is to be expected when the mutual impedance effects are large enough to dominate the reflecting screen factor.

The brightness temperature scale, which depends on beam shape as well as on forward gain, may be derived from the flux density calibration using the relation

$$T_b = \frac{S\lambda^2}{2k\Omega} \tag{4}$$

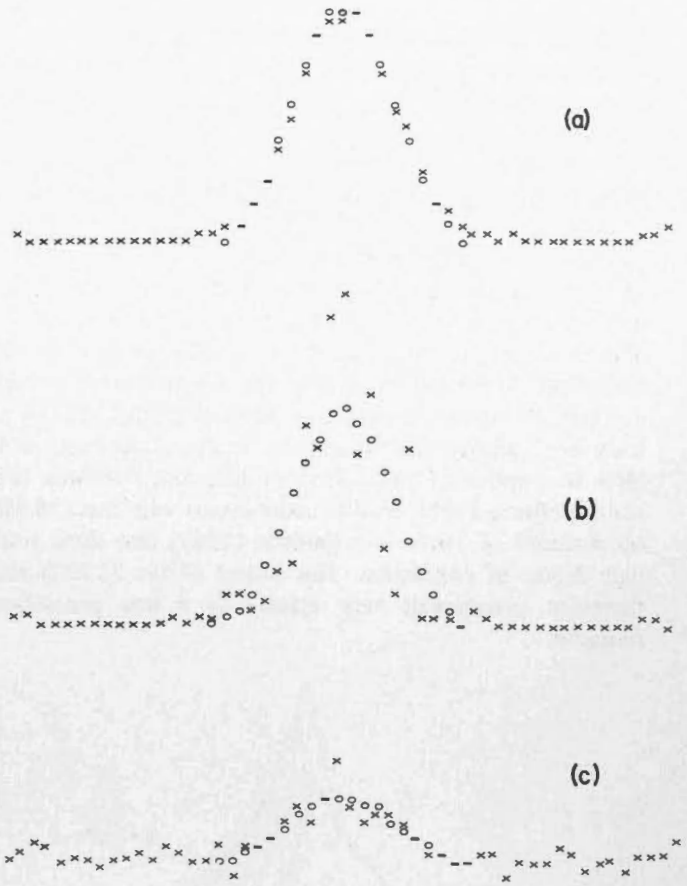

Figure 11. Facsimile of computer type-plots of three scans over point sources (X X X) with galactic background removed and theoretical beam shape (0 0 0) fitted (coincidence of X and 0 shown as –). (a) 3C 348, $S = 2690 \times 10^{-26}\,\mathrm{Wm^{-2}Hz^{-1}}$ (b) 3C 348, severe ionospheric scintillation. (c) 3C 190, $S = 50 \times 10^{-26}\,\mathrm{Wm^{-2}Hz^{-1}}$.

where $\Omega = \Omega_0/\cos Z$ is the effective solid angle of the instrument corrected for foreshortening. T_b is the brightness temperature of an extended source averaged over the system response and S is the flux density of the equivalent point source.

In general, the 22 MHz system has performed very much as expected. The beam shape, as indicated by observations of point sources, conforms very closely to the theoretical pattern. Figure 11 shows the computer reduction of three scans where the galactic background has been removed and the theoretical beam shape fitted: (a) 3C 348 ($S = 2690 \times 10^{-26}\,\mathrm{Wm^{-2}Hz^{-1}}$) under good observing conditions, (b) 3C 348 showing severe ionospheric scintillation, and (c) 3C 190 ($S = 50 \times 10^{-26}\,\mathrm{Wm^{-2}Hz^{-1}}$), a weaker source near the confusion limit.

The side-lobe responses are confined mainly to the two principal planes of the instrument. In hour angle, the first side-lobe is typically –3 to –4 per cent and the remainder are all less than 1 per cent, falling below the limit of detection (0.1 per cent) at angles greater than 10°. In declination, the first side-lobe is approximately –4 per cent and other nearby side-lobes are around 2 per cent or less. An examination of all available survey records for spurious responses in declination

from the intense sources, *Cassiopeia A* and *Virgo A*, revealed no values greater than 1 per cent for angles more than 18° away from the main beam and a mean absolute value of less than 0.5 per cent.

The response of the system to an extended source is illustrated in Figure 12. This shows a scan across the galactic plane at $\delta = -12\overset{\circ}{.}2$ ($Z = 61°0$). The comparison scan (dashed line) at $\delta = -12\overset{\circ}{.}9$ was taken with a 50 MHz array at Jicamarca, Peru, directed to the zenith (Ochs, 1966). This array is a simple square aperture with a beamwidth of 1°1. The intensity has been scaled to provide the best fit. The agreement is excellent except for regions near $\alpha = 18^h15^m$ and $\alpha = 16^h20^m$ where absorption by interstellar ionized hydrogen is clearly indicated. This absorption is also evident on the 4.7 MHz observations (dotted line) of Ellis and Hamilton (Ellis and Hamilton, 1966). Similar comparisons with the 178 MHz observations of Turtle and Baldwin (1962) also show a very high degree of correlation. The output of the 22 MHz array therefore corresponds very closely to a true pencil-beam response.

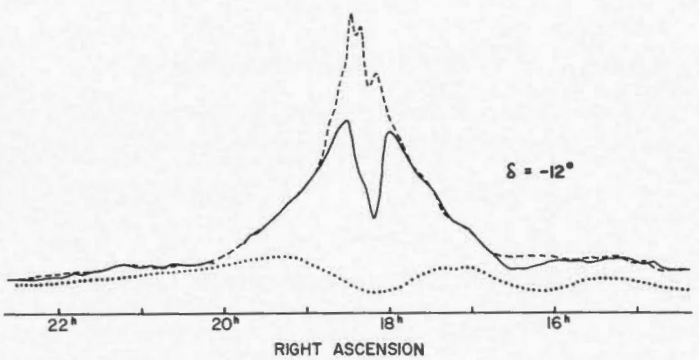

Figure 12. Scans across the galactic plane ($\delta = -12°$): ———22.25 MHz, ---- 50 MHz (Ochs, 1966), ... 4.7 MHz (Ellis and Hamilton, 1966) (not to scale).

Discussion

The performance of the array shows that the *T*-configuration may be used to produce a practical pencil-beam instrument. The declination side-lobes are small and the extra width of the N-S array has proven an effective means of suppressing the far-out side-lobes in hour angle. The sharing of the dipoles in the overlap region has resulted in an accurate total-power response.

It should be emphasized that the spurious responses of the system may be either positive or negative and have a mean value very near zero. The instrument is therefore largely free of the systematic bias that is present in the output of a conventional aperture where the side-lobe contribution is always positive.

The 22 MHz array has been in full operation since mid-1965 and is used primarily for two kinds of observations. First, drift scans of the type shown in Figure 12 have been made at half-beamwidth intervals and are being used to prepare a complete map of the northern sky from declination +90° to −20°. This will permit studies of the distribution of the thermal and nonthermal radiation from the galaxy. Secondly, several short scans of the type shown in Figure 11 have been made over the positions of each of about 400 radio sources. These results, coupled with the survey observations, will provide 22 MHz flux density measures for 400 to 500 sources down to a limiting flux density of 30 × 10^{-26} $Wm^{-2}Hz^{-1}$.

Acknowledgments

The authors would like to thank Dr. J.L. Locke and Dr. J.A. Galt for their help and encouragement during the design and construction of the array. Mr. J.H. Dawson assisted ably with the construction and maintenance of the receiver system.

References

Bazelyan, L.L., Braude, S.Ya., Vaisberg, V.V., Krymkin, V.V., Men', A.V., and Sodin, L.G., 1965. Study of the spectra of discrete sources of cosmic radio emission at frequencies below 40 Mc/s. *Soviet Astronomy-AJ*, Vol. 9, No. 3, pp 471-479.

Blythe, J.H., 1957. A new type of pencil-beam aerial for radio astronomy. *Monthly Notices Roy. Astron. Soc.*, Vol. 117, No. 6, pp 644-651.

Bracewell, R.N., and Swarup, G., 1961. The Stanford microwave spectroheliograph antenna, a microsteradian pencil-beam interferometer. *IRE Trans. Antennas and Prop.*, Vol. AP-9, pp 22-30.

Brouk, Yu,M., Goncharov, N. Yu, Men', A.V., Sodin, L.G., and Sharykin, N.K., 1967. T-form radio telescope with electrical beam scanning in 10-25 Mc/s range. *Radiofizika*, Vol. 10, No. 5, pp 608-619 (in Russian).

Costain, C.H., 1962. The new 22 Mc/s radio telescope of the Dominion Radio Astrophysical Observatory. Presented at the 1962 ASP Meeting, Victoria, Canada, *Publ. Astron. Soc. Pacific*, Vol. 74, No. 440, p 400.

Costain, C.H., and Smith, F.G., 1960. The radio telescope for 7.9 meters wavelength at the Mullard Observatory. *Monthly Notices Roy. Astron. Soc.*, Vol. 121, No. 4, pp 405-412.

Crowther, J.H., and Clarke, R.W., 1966. A pencil-beam radio telescope operating at 178 Mc/s. *Monthly Notices Roy. Astron. Soc.*, Vol. 132, No. 4.

Ellis, G.R.A., and Hamilton, P.A., 1966. Cosmic radio noise survey at 4.7 Mc/s. *Astrophys. J.*, Vol. 143, No. 1, pp 227-235.

Erickson, W.C., 1965. The decametric arrays at the Clarke Lake Radio Observatory. *IEEE Trans. Antennas and Propagation*, Vol. AP-13, No. 3, pp 422-427.

Galt, J.A., and Costain, C.H., 1965. Low frequency radio astronomy. *Trans. Roy. Soc. Can.*, Vol. 3, Series 4, pp 419-430.

Galt, J.A., Purton, C.R., and Scheuer, P.A.G., 1967. A large 10 MHz array for radio astronomy. *Pub. Dom. Obs.*, Vol. 25, No. 10, pp 295-304.

Gower, J.F.R., Scott, P.F., and Wills, D., 1967. A survey of radio sources in the declination ranges −07° to 20°, and 40° to 80°. *Memoirs Roy. Astron. Soc.*, Vol. 71, pp 49-144.

Kellermann, K.I., 1964. A compilation of radio source flux densities. *Pub. Owens Valley Radio Obs.*, Vol. 1, No. 1.

Little, A.G., 1958. Gain measurements of large radio telescope aerials. *Australian J. Phys.*, Vol. 11, No. 1, pp 70-78.

Mills, B.Y., 1963. Cross-type radio telescopes. *Proc. IRE (Australia)*, Vol. 24, No. 2, pp 132-140.

Mills, B.Y., Little, A.G., Sheridan, K.V., and Slee, O.B., 1958. A high resolution radio telescope for use at 3.5 m, *Proc. IRE*, Vol. 46, No. 1, pp 67-84.

Ochs, G.R., 1966. Synchrotron radiation measurements near the magnetic equator. In *Radiation Trapped in the Earth's Magnetic Field*, Billy M. McCormac, Ed., Dordrecht-Holland, D. Reidel Publishing Company, p 703.

Pauliny-Toth, I.I.K., Wade, C.M., and Heeschen, D.S., 1966. Positions and flux densities of radio sources. *Astrophys. J. Suppl.*, No. 116, Vol. 13, pp 65-124.

Pilkington, J.D.H., and Scott, P.F., 1965. A survey of radio sources between declinations 20° and 40°. *Memoirs Roy. Astron. Soc.*, Vol. 69, pp 183-224.

Ryle, M., 1952. A new radio interferometer and its application to the observations of weak radio stars. *Proc. Roy. Soc.*, A, Vol. 211, pp 351-375.

Ryle, M., and Hewish, A., 1960. The synthesis of large radio telescopes. *Monthly Notices Roy. Astron. Soc.*, Vol. 120, No. 3, pp 220-230.

Scott, P.F., Ryle, M., and Hewish, A., 1961. First results of radio star observations using the method of aperture synthesis. *Monthly Notices Roy. Astron. Soc.*, Vol. 122, No. 2, pp 95-111.

Shain, C.A., 1958. The Sydney 19.7 MC radio telescope. *Proc. IRE*, Vol. 46, No. 1, pp 85-88.

Shain, C.A., Komesaroff, M.M., and Higgins, C.S., 1961. A high resolution galactic survey at 19.7 Mc/s. *Australian J. Phys.*, Vol. 14, No. 4, pp 508-514.

Turtle, A.J., and Baldwin, J.E., 1962. A survey of galactic radiation at 178 Mc/s. *Monthly Notices Roy. Astron. Soc.*, Vol. 124, No. 6, pp 459-476.

Williams, P.J.S., Kenderdine, S., and Baldwin, J.E., 1966. A survey of radio sources and background radiation at 38 Mc/s. *Memoirs Roy. Astron. Soc.*, Vol. 70, pp 53-110.